PIER M

(Received 8 July 2025, Accepted 5 August 2025, Scheduled 13 August 2025)

CAMO-Net: A Channel Attention and Multi-Factor Optimized U-Net for Electromagnetic Inverse Scattering Problems

Tianhao Pan and Jianfa Liu*

College of Information Science and Electronic Engineering, Zhejiang University, Hangzhou 310058, China

ABSTRACT: Electromagnetic inverse scattering (EIS) problem is challenging due to its properties of strong nonlinearity and ill-posedness, where existing deep learning approaches often lack systematic network refinement and comprehensive analysis of key factors affecting performance. This work introduces CAMO-Net, a U-Net-based framework for EIS that integrates a channel-attention mechanism and systematically optimizes architectural and training factors to address these limitations. By integrating channel attention into skip connections, adopting a multi-scale channel configuration, and fine-tuning key hyperparameters through controlled experiments, CAMO-Net achieves superior accuracy and robustness. Experimental results demonstrate that it reduces the mean relative error (MRE) by 32.5% and the mean squared error (MSE) by 34.1% compared to the baseline U-Net. Our results demonstrate that joint channel attention and multi-factor optimization provide an effective, reproducible pathway for high-precision EIS imaging, offering new insights for robust reconstruction in EIS problems.

1. INTRODUCTION

Electromagnetic inverse scattering (EIS) [1, 2] plays a crucial role in applications such as biomedical imaging[3], geological exploration [4], target identification [5], and indoor positioning [6] aiming to recover the spatial distribution of electromagnetic parameters (e.g., permittivity) from measured scattered field data. However, EIS is inherently ill-posed and nonlinear [7], making high-precision and robust reconstruction extremely challenging — especially in the presence of noise and limited measurement data. Traditional physics-driven iterative algorithms, such as Contrast Source Inversion (CSI) [8] and Born Iterative Method (BIM) [9], offer clear physical interpretability but are hindered by high computational costs and slow convergence rates. These methods also struggle with noise sensitivity and require numerous iterations to achieve satisfactory results, which makes them less practical for large-scale or real-time applications.

On the other hand, non-iterative methods [2, 10, 11] such as those based on direct inversion or model-order reduction offer faster computational speeds but tend to suffer from lower accuracy, especially when reconstructing complex scattering environments or dealing with noisy data. While they are useful in some scenarios, their lack of adaptability to nonlinear problems and fine-scale details limits their applicability in precision-demanding contexts.

Recent advances in deep learning (DL) have demonstrated the potential to address some of these limitations by enabling end-to-end, efficient EIS reconstructions. U-Net and its variants [12], with their encoder-decoder architecture and skip connections, have achieved promising results in related image-to-image translation tasks. Nevertheless, current DL-based EIS approaches typically focus on architectural modifications at a macro level — such as introducing Transformer modules [13] — while neglecting a systematic investigation and refinement of internal network components and critical hyperparameters. This often leads to suboptimal exploitation of model capacity, insufficient robustness, and limited interpretability, particularly in reconstructing complex permittivity distributions with sharp boundaries, fine-scale features, and multi-material interfaces [14, 15]. Moreover, the lack of comprehensive analysis on how factors like channel attention mechanisms, feature channel configuration, loss functions, and training strategies interact to influence reconstruction quality remains an open issue in the field.

To address these gaps, a novel framework named CAMO-Net is proposed for high-precision electromagnetic inverse scattering (EIS) reconstruction. CAMO-Net systematically integrates a channel attention mechanism (CAM) into U-Net skip connections to adaptively enhance critical feature channels, while a multi-factor optimization framework rigorously investigates and tunes key architectural and training parameters through controlled experiments. This joint design not only improves quantitative metrics such as mean relative error and artifact suppression, but also delivers reproducible and robust reconstruction performance across diverse electromagnetic scenarios. The main contributions of this work are as follows:

1. A U-Net-based EIS reconstruction framework, CAMO-Net, is proposed, embedding channel attention in skip connections to enhance critical feature representation and suppress redundant information.

2. Key architectural and training factors — including channel configuration, depth, loss function design, and learning strategies — are systematically analyzed and optimized via con-

* Corresponding author: Jianfa Liu (12331091@zju.edu.cn).

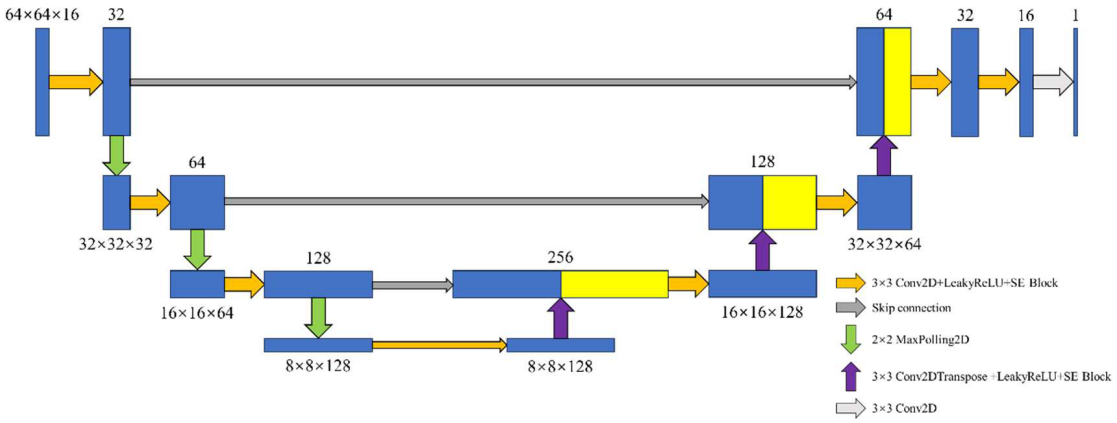

FIGURE 1. Schematic of CAMO-Net architecture.

trolled experiments, providing new insights into their coupling effects on EIS performance.

3. Experimental results demonstrate that CAMO-Net achieves significant improvements over baseline models in reconstruction accuracy, artifact suppression, and robustness, offering a reproducible pathway for high-precision EIS imaging in complex environments.

The rest of this paper is organized as follows. Section 2 details the problem formulation and CAMO-Net architecture. Section 3 presents comprehensive experimental results and ablation studies. Section 4 concludes with a discussion and future work.

2. METHODOLOGY

2.1. Problem Formulation

Electromagnetic inverse scattering (EIS) aims to reconstruct the spatial distribution of electromagnetic parameters (such as complex permittivity) from measurements of the scattered field generated by incident electromagnetic waves interacting with unknown targets [5]. This problem is fundamentally nonlinear and ill-posed, leading to non-unique and unstable solutions, especially under limited or noisy measurements. Conventionally, EIS is governed by the Lippmann-Schwinger equation, which describes the relationship among the incident field, the scattered field, and the target's permittivity distribution:

$$E^t(r) = E^i(r) + i\omega\mu_0 \int_D g(r,r') \left[-i\omega\epsilon_0(\epsilon_r(r')-1)E^t(r')\right] dr', r \in D \quad (1)$$

$$E^s(r) = i\omega\mu_0 \int_D g(r,r') \left[-i\omega\epsilon_0(\epsilon_r(r')-1)E^t(r')\right] dr', r \in S \quad (2)$$

where E^t and E^i denote the total and incident electric fields; $g(r,r')$ is the free-space Green's function; and ϵ_r is the target's complex relative permittivity. The goal is to recover $\epsilon_r(r)$ across the domain D from scattered field measurements E^s taken on an observation surface S.

Traditional physics-driven iterative algorithms (e.g., CSI [8], BIM [9], and subspace-based optimization method (SOM) [17]) solve this problem by repeatedly updating ϵ_r based on the discrepancy between simulated and measured data, but these approaches are computationally costly and often sensitive to modeling errors. Recent advances in deep learning enable direct, end-to-end mapping from E^s to ϵ_r with high efficiency. However, existing data-driven models frequently underperform when reconstructing fine structural details or in the presence of artifacts, due to insufficiently optimized network architectures and lack of systematic hyperparameter analysis [13–15].

2.2. CAMO-Net Architecture

To overcome the limitations of both traditional and previous deep learning-based EIS reconstruction methods, a novel U-Net-based framework named CAMO-Net is proposed (see Figure 1), featuring channel attention and multi-factor optimization. The core architecture adopts an encoder-decoder structure with skip connections, enabling efficient multi-scale feature fusion and rapid end-to-end reconstruction of permittivity maps. CAMO-Net differentiates itself by strategically embedding a channel attention mechanism (CAM) in skip connections and by systematically optimizing architectural and training factors through rigorous ablation and controlled studies. While Jin et al. [17] utilized physics-inspired networks to solve phase retrieval in holographic metasurfaces, our approach extends this paradigm by integrating channel attention and multi-factor optimization specifically for EIS problems, addressing the unique challenges of nonlinear permittivity reconstruction.

2.2.1. Channel Attention Mechanism

A key innovation in CAMO-Net is the introduction of a channel attention mechanism (CAM) within the skip connections, as visualized in Figure 2. For each skip pathway, CAM adaptively recalibrates feature channels by learning their relative importance, thus amplifying discriminative information crucial for reconstructing boundaries, small-scale targets, and multi-material interfaces. Figure 2 illustrates how this is achieved through [18]:

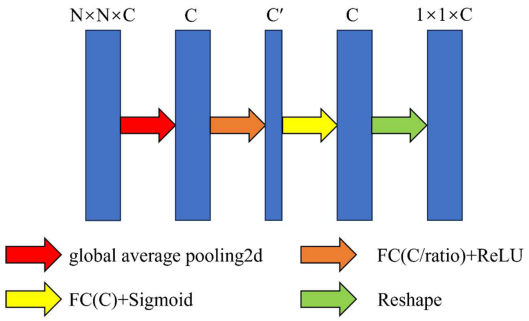

FIGURE 2. Visualization of channel attention integration.

1. **Global Average Pooling**: For a feature map $F \in R^{C\times H\times W}$, spatial averaging produces a channel descriptor $z \in R^C$:

$$z_c = \frac{1}{H \times W} \sum_{i=1}^{H} \sum_{j=1}^{W} F_c(i,j) \tag{3}$$

2. **Attention Weight Generation**: A multilayer perceptron (MLP) with nonlinear activations (rectified linear unit (ReLU), Sigmoid) and dimensionality reduction ratio r outputs the attention weights $s \in R^C$:

$$s = \sigma(W_1 \delta(W_0 z)) \tag{4}$$

where W_0, W_1 are trainable parameters; δ is the ReLU; and σ is the Sigmoid.

3. **Channel Re-Weighting**: The channel attention weights are applied to F:

$$\tilde{F}_c = s_c \cdot F_c \tag{5}$$

By embedding CAM at each skip connection, CAMO-Net selectively strengthens important feature channels and suppresses redundant or noisy information. Similar to the complex-baseband frequency modulated continuous wave (FMCW) radar in [19], which avoids image-band noise folding through quadrature mixing, our CAM adaptively re-weights feature channels to enhance critical signals while suppressing noise. This design directly addresses issues of detail loss and artifact introduction prevalent in standard U-Net and other DL-based EIS models [20]. This design is particularly effective in enhancing the recovery of complex permittivity distributions.

The practical impact of this innovation lies in its ability to enhance the recovery of sharp boundaries and small-scale targets, which are typically difficult to capture using conventional models. This is crucial in applications like biomedical imaging and geological exploration, where accurate, high-resolution reconstructions are essential.

However, there are also limitations to this approach. The introduction of channel attention increases computational complexity, adding overhead that may slow down training and inference, especially when handling large-scale or high-resolution data. Furthermore, the model's performance is sensitive to hyperparameter tuning, and the process of selecting optimal configurations for the attention mechanism, activations, and dimensionality reduction ratios can be time-consuming and resource-intensive.

2.2.2. Multi-Factor Optimization

CAMO-Net's performance is further boosted by a systematic, multi-factor optimization framework that investigates and tunes critical architectural and training parameters. Specifically:

1. **Optimize Channel Configuration**: Explore and adopt a pyramid-shaped multi-scale channel configuration, enabling shallow layers to focus on fine low-level details and deeper layers to encode richer semantic information, thereby facilitating accurate feature fusion across scales [14].

2. **Depth Selection**: Empirically determine the optimal encoder-decoder depth, balancing model expressivity and generalization while controlling overfitting.

3. **Loss Function Design**: Employ a composite loss combining mean squared error (MSE) and structural similarity index measure (SSIM) to promote both pixel-level accuracy and structural fidelity [21]:

$$\text{Loss} = \lambda_1 \cdot \text{MSE} + (1-\lambda_1) \cdot \text{SSIM} \tag{6}$$

where λ_1 is the loss coefficient controlling the priority of the MSE.

4. **Training Strategy**: Systematically evaluate the effects of learning rate (η) scheduling, batch size (B), and activation functions (LeakyReLU) to maximize reconstruction robustness and convergence speed.

Through rigorous ablation and controlled experiments, CAMO-Net demonstrates substantial quantitative and qualitative improvements over baseline models, including lower mean relative error and superior artifact suppression. This joint channel attention and multi-factor optimization framework thus provides a reliable, reproducible pathway for high-precision EIS imaging, robust to diverse and challenging electromagnetic scenarios.

3. EXPERIMENTS

Comprehensive experiments are conducted to evaluate the performance of CAMO-Net in EIS reconstruction, systematically comparing it with baseline methods, conducting ablation studies, and analyzing parameter sensitivity.

3.1. Setup

All experiments are performed on Ubuntu 22.04 LTS with NVIDIA GeForce RTX 4090 GPUs and TensorFlow 2.11.0. The dataset includes 2D permittivity distributions and their corresponding scattered field measurements, generated using the forward model outlined in Section 2. It covers a broad spectrum of target geometries and material properties (including varying complex permittivity values). To ensure the model's generalization capability, the training data incorporates diverse noise levels and measurement errors, reflecting real-world conditions and enhancing the model's robustness across different scenarios. The network is trained with early stopping (patience = 10,

monitoring validation loss) to ensure convergence and prevent overfitting.

In all results, the relative permittivity is scaled according to the equation $\varepsilon_r = (\varepsilon_r^o - 1) * C$ where ε_r and ε_r^o, and C denote scaled relative permittivity, relative permittivity, and constant coefficient ($C = 10$ in this work), respectively. The performance is evaluated using mean relative error (MRE), mean squared error (MSE), and their respective reduction rates, as defined:

$$\text{MRE} = \frac{1}{N}\sum_{i=1}^{N}\frac{|\varepsilon_r^t - \varepsilon_r^r|_F}{|\varepsilon_r^t|_F} \tag{7}$$

$$\text{MSE} = \frac{1}{N}\sum_{i=1}^{N}|\varepsilon_r^t - \varepsilon_r^r|_F^2 \tag{8}$$

$$\text{MRE Reduction Ratio} = 1 - \frac{\text{MRE}_{\text{output}}}{MRE_{\text{input}}} \tag{9}$$

$$\text{MSE Reduction Ratio} = 1 - \frac{\text{MSE}_{\text{output}}}{MSE_{\text{input}}} \tag{10}$$

where ε_r^t and ε_r^r denote the ground-truth and reconstructed scaled relative permittivity profiles, respectively, and N is the number of test samples. Unless otherwise specified, all experiments use the hyperparameters summarized in Table 1.

TABLE 1. Baseline hyperparameter configurations.

Parameter	Image Resolution	Input/Output Channels	Kernel Size	Learning Rate	Batch Size
Value	64×64	16/1	3×3	1e-4	5

3.2. Performance Comparison with Different Models

To validate the effectiveness of CAMO-Net's integrated channel attention mechanism and multi-factor optimization strategy, a direct performance comparison is conducted with the baseline U-Net model and other representative methods (long short-term memory (LSTM) [22], MLP [23]) on the EIS reconstruction task. As shown in Table 2, CAMO-Net achieves substantial improvements, reducing MRE by 32.54% and MSE by 34.05% over the baseline. Although the per-epoch processing time has moderately increased, the computational efficiency remains comparable. This significant gain highlights its effectiveness in addressing the nonlinearity and ill-posedness of EIS reconstruction. The results confirm CAMO-Net's superior capability to recover complex permittivity distributions, suppress artifacts, and enhance robustness compared to standard U-Net. Meanwhile, LSTM and MLP models show limited performance. LSTM exhibits higher MRE and MSE due to its sequential dependency constraints, while MLP, though faster, fails to capture the nonlinear correlations in EIS data, resulting in larger errors.

Figure 3 presents visual reconstructions that demonstrate CAMO-Net's advantages in recovering complex permittivity distributions, suppressing background artifacts, and enhancing robustness compared to standard U-Net.

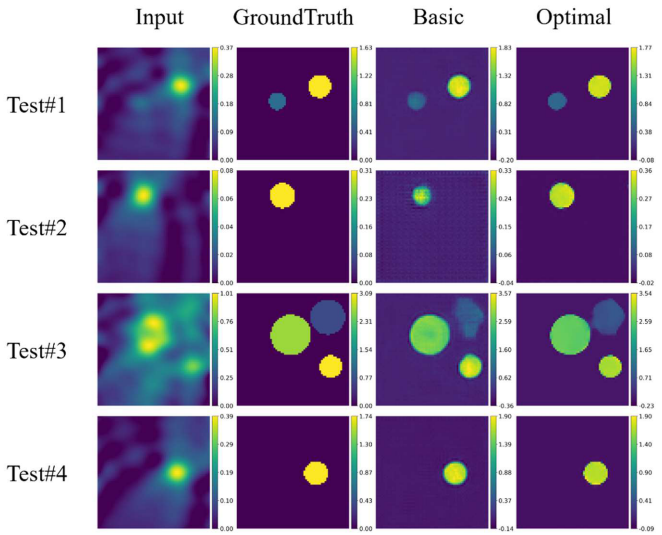

FIGURE 3. Visualization of scaled relative permittivity reconstruction results.

3.3. Ablation Studies

Ablation studies are conducted to systematically evaluate the contributions of individual architectural components within CAMO-Net, focusing on its most critical elements.

3.3.1. Ablation with Compression Ratio

The impact of varying the channel attention compression ratio $r \in 2, 4, 8$ in skip connections is systematically evaluated. As shown in Table 3, $r = 4$ achieves the best trade-off, yielding the greatest improvement in MRE and MSE over the baseline. Lower or higher ratios either insufficiently capture inter-channel dependencies or introduce information loss, respectively. Besides, embedding CAM with $r = 4$ notably enhances edge and texture reconstruction, as visualized in Figure 4.

3.3.2. Ablation with Channel Configuration and Network Depth

The influence of channel configuration variations (Narrow, Wide, Pyramid) and network depth (2, 3, 4 layers) is systematically examined under the optimal channel attention compression setting ($r = 4$). Table 4 shows that the pyramid configuration yields the lowest MRE, balancing multi-scale feature extraction and facilitating accurate recovery of both large-scale and fine-grained EIS structures. Figure 5 showcases its effectiveness in reconstructing targets of varying sizes.

Table 5 summarizes the results with different encoder-decoder depths. A 3-layer structure provides optimal performance, with deeper models showing diminishing returns and potential overfitting.

3.4. Parameter Sensitivity Studies

This section presents a systematic analysis of parameter sensitivity concerning the loss function coefficient λ_1 and training strategies (learning rate η, batch size B, activation function), further optimizing model robustness.

TABLE 2. Performance comparison with different models.

Models	MRE			MSE			TIME	
	Max	Min	Mean	Max	Min	Mean	Mean	Total
Baseline	1.0107	0.1378	0.2371	0.1227	0.3760e-3	0.0338	1.47s	230.8s
LSTM	1.4269	0.3698	0.5707	0.8142	0.7502e-3	0.2226	2.86s	251.3s
MLP	1.0879	0.3590	0.5197	0.5849	0.4361e-3	0.1981	1.01s	86.8s
CAMO-Net	0.3938	0.0778	0.1599	0.1085	0.0336e-3	0.0223	2.92s	248.1s

TABLE 3. Comparison of CAM compression ratios.

Metrics		MRE	Reduction Ratio	MSE	Reduction Ratio
Baseline		0.2371	70.40%	0.0338	93.53%
r	2	0.2207	72.44%	0.0302	94.21%
	4	0.2176	72.84%	0.0297	94.32%
	8	0.2179	72.79%	0.0309	94.09%

TABLE 4. Comparison of feature channel configuration types.

Metrics		MRE	Reduction Ratio	MSE	Reduction Ratio
Baseline		0.2371	70.40%	0.0338	93.53%
Channel Type	Narrow	0.2562	68.01%	0.0390	92.53%
	Wide	0.2210	72.40%	0.0314	93.98%
	Pyramid	0.2134	73.36%	0.0285	94.54%

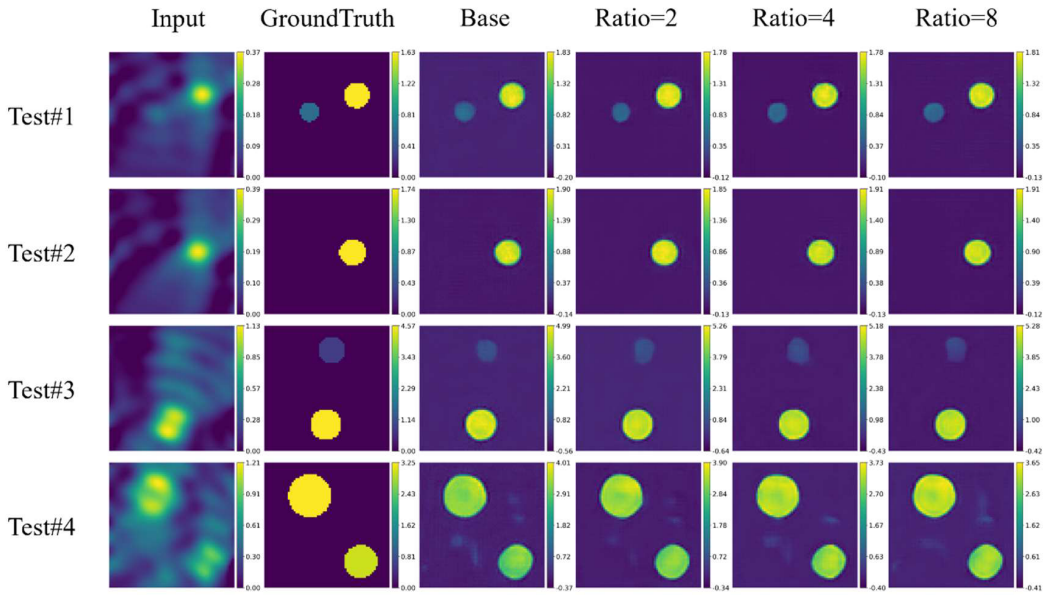

FIGURE 4. Visualization of scaled relative permittivity reconstruction results with varying compression ratios r.

3.4.1. On Loss Coefficients

The impact of the composite loss function coefficient λ_1 is investigated in Table 6. $\lambda_1 = 0.4$ yields the best overall result, reducing MRE by 4.50%. This demonstrates that combining pixel-wise and structural losses enhances the preservation of fine details and structural fidelity in EIS reconstructions, as further visualized in Figure 6.

3.4.2. On Training Strategy Hyperparameters

The influence of learning rate (η), batch size (B), and LeakyReLU negative slope coefficient (α) on model performance is systematically evaluated through controlled experiments.

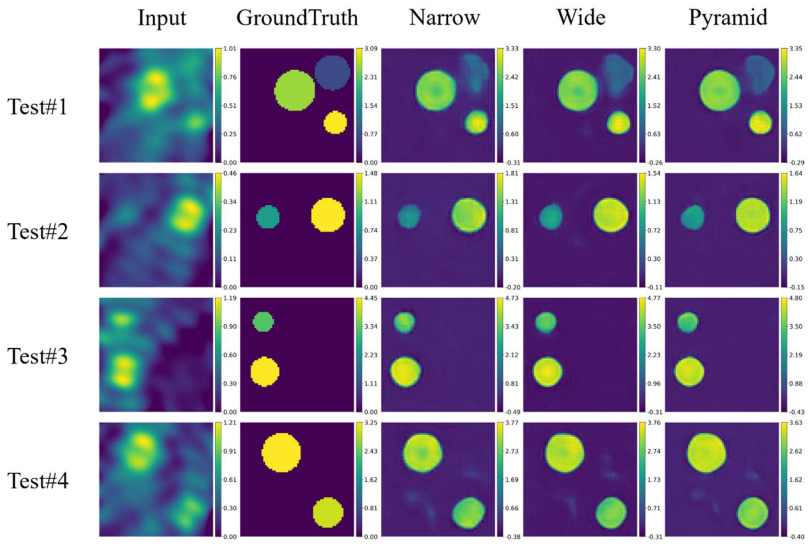

FIGURE 5. Visualization of scaled relative permittivity reconstruction results with different channel configurations.

TABLE 5. Comparison of encoder/decoder depths.

Metrics		MRE	Reduction Ratio	MSE	Reduction Ratio
Baseline		0.2371	70.40%	0.0338	93.53%
# layers	2	0.2134	73.36%	0.0285	94.54%
	3	0.1894	76.35%	0.0242	95.36%
	4	0.2207	72.45%	0.0326	93.77%

TABLE 6. Performance under different loss function coefficients λ_1.

Metrics		MRE	Reduction Ratio	MSE	Reduction Ratio
Baseline		0.2371	70.40%	0.0338	93.53%
λ_1	0.5	0.1857	76.82%	0.0269	94.84%
	0.4	0.1809	77.41%	0.0259	95.03%
	0.3	0.1963	75.49%	0.0298	94.29%

TABLE 7. Performance under different learning rate settings.

Metrics		MRE	Reduction Ratio	MSE	Reduction Ratio
Baseline		0.2371	70.40%	0.0338	93.53%
η	1e-3	0.1765	77.96%	0.0250	95.21%
	5e-4	0.1767	77.93%	0.0238	95.44%
	1e-4	0.1809	77.41%	0.0259	95.03%
	1e-3 with Scheduler	0.1685	78.96%	0.0257	95.07%

TABLE 8. Performance under different batch sizes.

Metrics		MRE	Reduction Ratio	MSE	Reduction Ratio
Baseline		0.2371	70.40%	0.0338	93.53%
B	1	0.1769	77.91%	0.0271	94.81%
	4	0.1739	78.29%	0.0249	95.22%
	6	0.1621	79.76%	0.0239	95.42%
	8	0.1681	79.02%	0.0250	95.22%

TABLE 9. Impact of leakyReLU negative slope coefficient α.

Metrics		MRE	Reduction Ratio	MSE	Reduction Ratio
Baseline		0.2371	70.40%	0.0338	93.53%
α	0.1	0.1711	78.63%	0.0231	95.57%
	0.2	0.1599	80.03%	0.0223	95.73%
	0.3	0.1606	79.94%	0.0227	95.65%

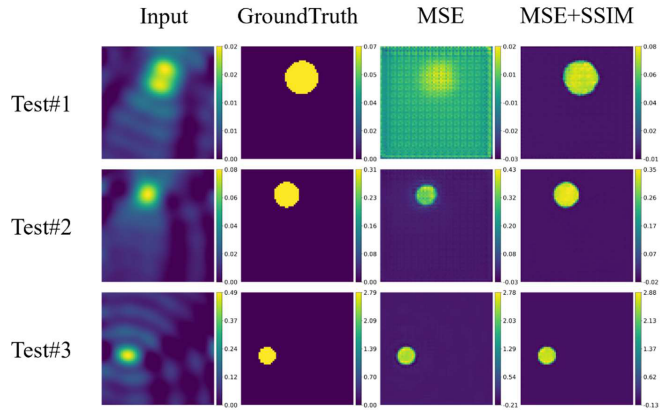

FIGURE 6. Visualization of scaled relative permittivity reconstruction with different loss functions.

Table 7 shows that the dynamic learning rate scheduler achieves the lowest MRE and best convergence, showing its effectiveness for robust convergence in EIS reconstruction.

Table 8 reveals that batch size 6 provides the best trade-off; too small or too large batch sizes degrade performance due to instability or loss of sharpness.

Table 9 indicates that LeakyReLU with $\alpha = 0.2$ delivers the lowest MRE, owing to improved gradient flow and robustness in weak-signal regions.

4. CONCLUSION

This work presents CAMO-Net, a systematically optimized U-Net framework that incorporates channel attention mechanisms and multi-factor architectural refinements to address fundamental challenges in electromagnetic inverse scattering (EIS), including its inherent nonlinearity, ill-posed nature, and susceptibility to noise. By embedding channel attention modules within skip connections and rigorously tuning key factors such as channel configuration, network depth, loss function design, and training strategies, CAMO-Net demonstrates significant improvements in both reconstruction accuracy and robustness. Our experiments show that CAMO-Net achieves up to 32.54% reduction in mean relative error and 34.05% reduction in mean squared error compared to standard U-Net baselines, while also providing superior artifact suppression and recovery of complex permittivity distributions. In comparisons with other representative methods (LSTM, MLP), although MLP is faster in training speed, it fails to capture the nonlinear correlations inherent in EIS data, leading to larger reconstruction errors. The systematic ablation studies further clarify the independent and joint contributions of each optimization, underscoring the reproducibility and reliability of our approach in diverse and challenging EIS scenarios.

Despite these advances, several limitations remain. While CAMO-Net substantially improves performance for 2D EIS problems, its current design does not directly address 3D reconstruction [24] or scenarios with extremely sparse or low-SNR measurements. Furthermore, the integration of explicit physical constraints, such as differentiable Lippmann-Schwinger solvers, remains a promising direction to further enhance generalization and interpretability. Future work will focus on extending CAMO-Net to 3D EIS, exploring robustness under harsher noise or data scarcity conditions, and fusing the optimized architecture with physics-driven models [25] to push high-precision electromagnetic imaging toward even more challenging real-world applications.

REFERENCES

[1] Cakoni, F. and D. Colton, "Combined far-ield operators in electromagnetic inverse scattering theory," *Mathematical Methods in the Applied Sciences*, Vol. 26, No. 5, 413–429, 2003.

[2] Yin, T., Z. Wei, and X. Chen, "Non-iterative methods based on singular value decomposition for inverse scattering problems," *IEEE Transactions on Antennas and Propagation*, Vol. 68, No. 6, 4764–4773, 2020.

[3] Radke, K. L., B. Kamp, V. Adriaenssens, J. Stabinska, P. Gallinnis, H.-J. Wittsack, G. Antoch, and A. Müller-Lutz, "Deep learning-based denoising of CEST MR data: A feasibility study on applying synthetic phantoms in medical imaging," *Diagnostics*, Vol. 13, No. 21, 3326, 2023.

[4] Fan, G., F. Chen, D. Chen, Y. Li, and Y. Dong, "A deep learning model for quick and accurate rock recognition with smartphones," *Mobile Information Systems*, Vol. 2020, No. 1, 7462524, 2020.

[5] Wen, Z., D. Liu, X. Liu, L. Zhong, Y. Lv, and Y. Jia, "Deep learning based smart radar vision system for object recognition," *Journal of Ambient Intelligence and Humanized Computing*, Vol. 10, No. 3, 829–839, 2019.

[6] Wang, Q., A. H. Paulus, M. S. Tong, and T. F. Eibert, "An indoor localization technique utilizing passive tags and 3-D microwave passive radar imaging," *Progress In Electromagnetics Research*, Vol. 181, 89–98, 2024.

[7] Chen, X., *Computational Methods for Electromagnetic Inverse Scattering*, John Wiley & Sons, 2018.

[8] Van Den Berg, P. M. and R. E. Kleinman, "A contrast source inversion method," *Inverse Problems*, Vol. 13, No. 6, 1607, 1997.

[9] Zhang, W. and A. Hoorfar, "Reconstruction of two-dimensional permittivity distribution with distorted rytov iterative method," *IEEE Antennas and Wireless Propagation Letters*, Vol. 10, 1072–1075, 2011.

[10] Devaney, A. J., "Inverse-scattering theory within the Rytov approximation," *Optics Letters*, Vol. 6, No. 8, 374–376, 1981.

[11] Habashy, T. M., R. W. Groom, and B. R. Spies, "Beyond the born and rytov approximations: A nonlinear approach to electromagnetic scattering," *Journal of Geophysical Research: Solid Earth*, Vol. 98, No. B2, 1759–1775, 1993.

[12] Wang, Y., Z. Zong, S. He, R. Song, and Z. Wei, "Push the generalization limitation of learning approaches by multidomain weight-sharing for full-wave inverse scattering," *IEEE Transactions on Geoscience and Remote Sensing*, Vol. 61, 1–14, 2023.

[13] Sun, G., Y. Pan, W. Kong, Z. Xu, J. Ma, T. Racharak, L.-M. Nguyen, and J. Xin, "Da-transunet: Integrating spatial and channel dual attention with transformer u-net for medical image segmentation," *Frontiers in Bioengineering and Biotechnology*, Vol. 12, 1398237, 2024.

[14] Haberman, B., "Uniqueness in calderón's problem for conductivities with unbounded gradient," *Communications in Mathematical Physics*, Vol. 340, No. 2, 639–659, 2015.

[15] Guo, R., T. Huang, M. Li, H. Zhang, and Y. C. Eldar, "Physics-embedded machine learning for electromagnetic data imaging: Examining three types of data-driven imaging methods," *IEEE Signal Processing Magazine*, Vol. 40, No. 2, 18–31, 2023.

[16] Chen, X., "Subspace-based optimization method for solving inverse-scattering problems," *IEEE Transactions on Geoscience and Remote Sensing*, Vol. 48, No. 1, 42–49, 2010.

[17] Jin, L., J. Xie, B. Pan, and G. Luo, "Generalized phase retrieval model based on physics-inspired network for holographic metasurface (invited paper)," *Progress In Electromagnetics Research*, Vol. 178, 103–110, 2023.

[18] Wang, Q., B. Wu, P. Zhu, P. Li, W. Zuo, and Q. Hu, "ECA-Net: Efficient channel attention for deep convolutional neural networks," in *2020 IEEE/CVF Conference on Computer Vision and Pattern Recognition (CVPR)*, 11 531–11 539, Seattle, WA, USA, 2020.

[19] Hegazy, A. M., Hegazy, M. Alizadeh, A. Samir, M. Basha, and S. Safavi-Naeini, "Remote material characterization with complex baseband FMCW radar sensors," *Progress In Electromagnetics Research*, Vol. 177, 107–126, 2023.

[20] Hu, J., L. Shen, and G. Sun, "Squeeze-and-excitation networks," in *2018 IEEE/CVF Conference on Computer Vision and Pattern Recognition*, 7132–7141, Salt Lake City, UT, USA, 2018.

[21] Xia, Y. and S. He, "A lightweight deep learning model for full-wave nonlinear inverse scattering problems," *Progress In Electromagnetics Research M*, Vol. 128, 83–88, 2024.

[22] Hochreiter, S. and J. Schmidhuber, "Long short-term memory," *Neural Computation*, Vol. 9, No. 8, 1735–1780, 1997.

[23] Krizhevsky, A., I. Sutskever, and G. E. Hinton, "Imagenet classification with deep convolutional neural networks," *Communications of the ACM*, Vol. 60, No. 6, 84–90, 2017.

[24] Liu, J., Y. Wang, L. Jin, B. Wang, Z. Zong, S. He, and Z. Wei, "Exploring scaling laws in large learning models for inverse scattering with spatial-temporal diffusion," *IEEE Transactions on Antennas and Propagation*, 2025.

[25] Wei, Z. and X. Chen, "Physics-inspired convolutional neural network for solving full-wave inverse scattering problems," *IEEE Transactions on Antennas and Propagation*, Vol. 67, No. 9, 6138–6148, 2019.